Published OnlineFirst January 27, 2014; DOI: 10.1158/2159-8290.CD-13-0633

A

Sample	Age	Sex	Stage	Smoking status	AD subtype
Index-case	64	Female	Ib	Never	Invasive mucinous
Case-A	73	Female	Ia	Never	Invasive mucinous
Case-B	72	Female	Ia	Never	Invasive mucinous
Case-C	66	Female	Ia	Never	Invasive mucinous
Case-D	31	Female	Ia	Never	Invasive mucinous

EGFR, KRAS, BRAF, HER2, ALK, ROS, RET negative

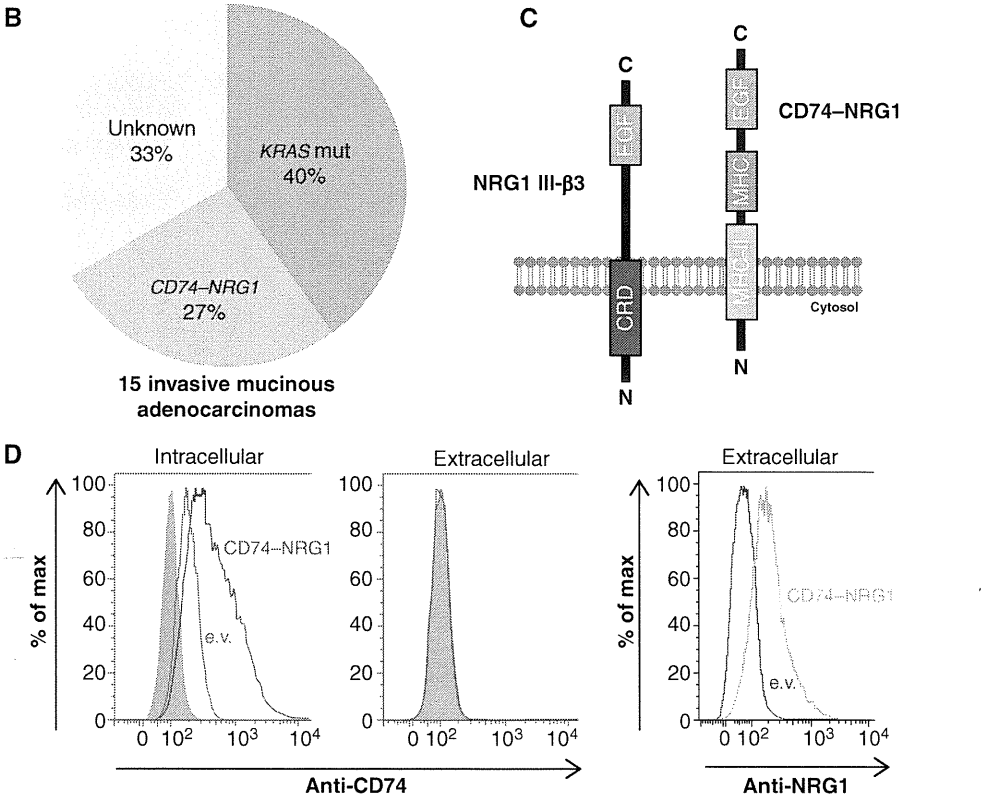

Figure 2. Association of *CD74–NRG1* with invasive mucinous adenocarcinoma, and membrane localization of the fusion protein. **A,** clinical characteristics of the index case and the 4 additional cases found to harbor *CD74–NRG1*. **B,** frequency of *KRAS* mutations and *CD74–NRG1* rearrangements in a cohort of 15 IMA tumors (East Asian population). **C,** schematic representation of wild-type NRG1 III-β3 and predicted CD74–NRG1 fusion protein in the cellular membrane. **D,** intracellular and extracellular staining of CD74 (left), and extracellular staining of NRG1 (right) in CD74–NRG1-transduced NIH-3T3 cells, detected by flow cytometry. The percentage of max is the number of cells in each bin divided by the number of cells in the bin that contains the largest number of cells. e.v., empty vector control.

(FPKM = 22.8; Fig. 3A; Supplementary Table S8) and also phosphorylated (Fig. 3B, right). *ERBB4* was not expressed in the index case (FPKM = 0.2; Fig. 3A; Supplementary Table S8). To our surprise, expression of phosphorylated ERBB3 (p-ERBB3) was almost exclusively restricted to fusion-positive cases, as determined by an immunohistochemical analysis of a tissue microarray containing 241 unselected adenocarcinomas. Although a positive signal was detected for p-ERBB3 in the five CD74–NRG1-positive invasive mucinous adenocarcinomas, only six of 241 unselected adenocarcinomas exhibited detectable levels of p-ERBB3 ($P < 0.0001$; Fig. 3C). Together, these observations support the notion that CD74–NRG1 might provide the ligand for ERBB2–ERBB3 heterodimers, thus activating the phosphoinositide 3-kinase (PI3K)–AKT pathway, as previously shown for wild-type NRG1 (16).

To formally test this hypothesis, we transduced different cell lines with retroviruses encoding CD74–NRG1 and performed Western blot analyses under starving conditions. Because NIH-3T3 cells have low-to-absent expression of ERBB receptors, and NIH-3T3 cells ectopically expressing ERBB2 and ERBB3 are already oncogenic (Supplementary Fig. S5), we decided to use H322 and H1568 lung cancer cell lines expressing normal ERBB2 and ERBB3 levels instead. We transduced these cell lines with either an empty vector, a virus containing the full fusion transcript, or a virus containing a truncated version of the fusion lacking the EGF-like domain (Supplementary Fig. S6). We observed that H322 and H1568 cell lines ectopically expressing CD74–NRG1 showed increased levels of p-ERBB2, p-ERBB3, p-AKT, and p-S6K when compared with the empty vector control (Fig. 3D). Furthermore, both p-ERBB3 and

Published OnlineFirst January 27, 2014; DOI: 10.1158/2159-8290.CD-13-0633

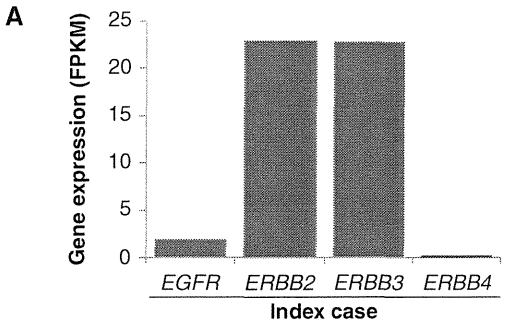

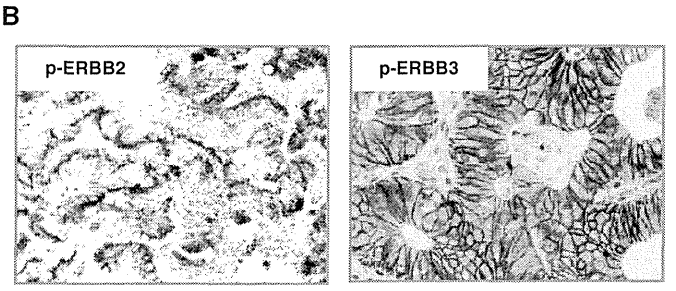

C

p-ERBB3	*CD74–NRG1* (*n* = 5)	AD cohort (*n* = 241)
Positive	5	6
Negative	0	235
		***P* < 0.0001**

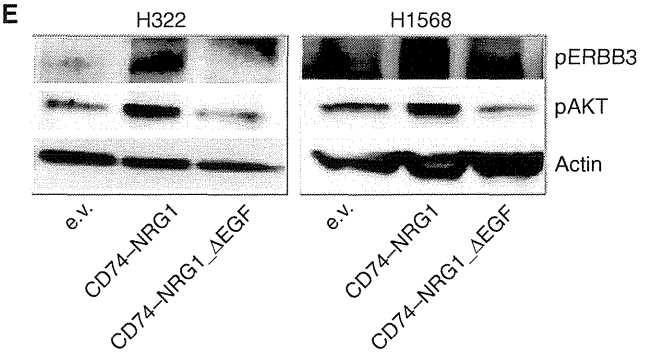

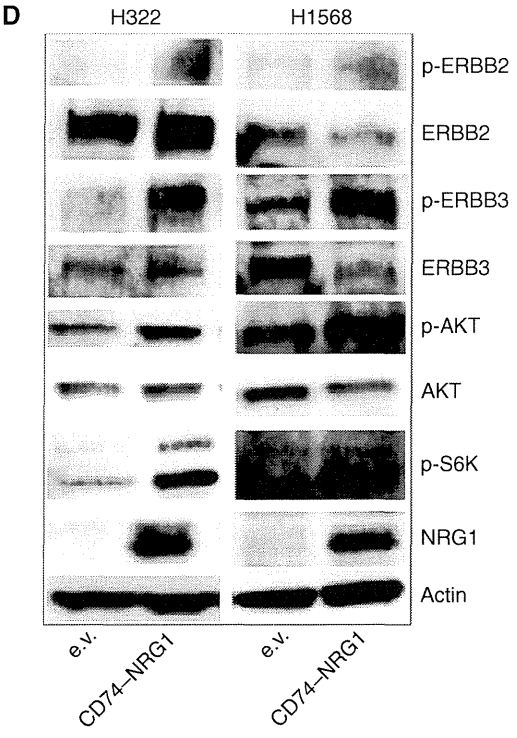

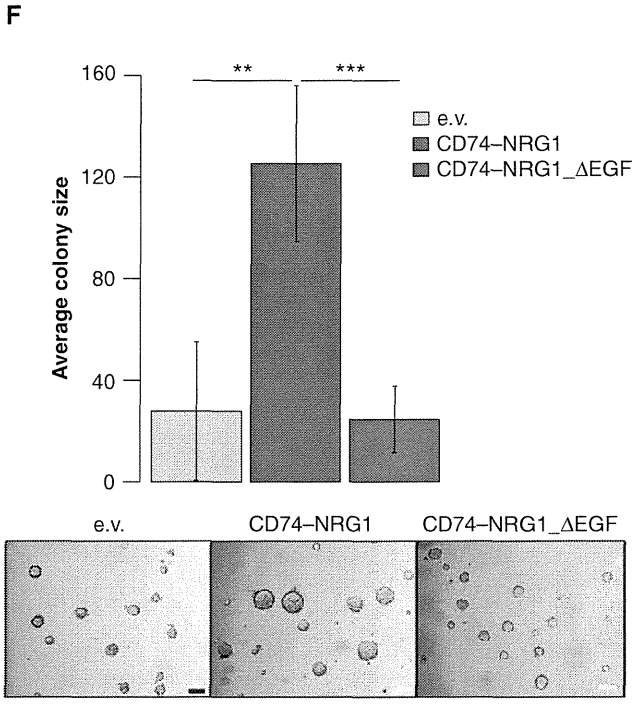

Figure 3. Functional relevance of CD74-NRG1. **A,** expression levels of ERBB receptors in the index case inferred from transcriptome sequencing data. FPKM values are shown. **B,** levels of p-ERBB2 and p-ERBB3 detected by immunohistochemical analysis in a CD74-NRG1-positive case using and antibody directed against ERBB2 Tyr1221/1222 and ERBB2 Tyr1289. **C,** the same p-ERBB3 antibody was used to stain a tissue microarray composed of 241 lung adenocarcinomas. The frequency of p-ERBB3-positive cases in this cohort versus the five CD74-NRG1-positive samples is shown ($P < 0.0001$). **D,** activation of the PI3K-AKT pathway detected by Western blot analysis of H322 and H1568 lung cancer cells transduced with retroviruses encoding CD74-NRG1 or the empty vector control (e.v.). **E,** levels of p-ERBB3 and p-AKT measured by Western blot analysis in the presence of an empty vector, CD74-NRG1, or a truncated version lacking the EGF-like domain (CD74-NRG1_ΔEGF). **F,** anchorage-independent growth of H1568 cells expressing an empty vector, CD74-NRG1, or a truncated version lacking the EGF-like domain (CD74-NRG1_ΔEGF). Top, the average colony size for the three conditions, with error bars representing standard deviations. The experiment was performed with two independent transductions for a total of four times. **, $P < 0.01$; ***, $P < 0.001$. Bottom, representative pictures of the colony formation assay. Please note that H1568 cells are oncogenic and form small colonies without any manipulation.

Published OnlineFirst January 27, 2014; DOI: 10.1158/2159-8290.CD-13-0633

p-AKT depended on the presence of the EGF-like domain of CD74–NRG1 in the fusion (Fig. 3E). In addition, coculture of NIH-3T3 cells ectopically expressing CD74–NRG1 with Ba/F3 cells genetically engineered to express normal ERBB2 and ERBB3 levels also led to activation of AKT (Supplementary Fig. S7). Finally, H1568 cells ectopically expressing CD74–NRG1 exhibited enhanced colony formation in soft-agar assays (Fig. 3F; Supplementary Table S9). Taken together, these data suggest that CD74–NRG1 leads to overexpression of the EGF-like domain of NRG1 III-β3 that acts as a ligand for ERBB3, inducing its phosphorylation and subsequent activation of the downstream PI3K–AKT pathway.

DISCUSSION

We have discovered *CD74–NRG1*, a novel recurrent fusion gene in lung adenocarcinoma that arises from a somatic genomic event. Taking into account the frequencies of mutations of *EGFR* (11.3%), *KRAS* (32.2%), *BRAF* (7%), *ERBB2* (1.7%), or fusions affecting *ALK* (1.3%), *ROS* (1.7%), and *RET* (0.9%; refs. 17, 18) in lung adenocarcinomas, for which our cohort was negative, and the fact that we found 4 positive cases in our validation cohort of 102 pan-negative lung adenocarcinomas, we estimate that the frequency of *CD74–NRG1* in lung adenocarcinomas is approximately 1.7%; however, it is of note that our validation cohort was from an Asian population, so this frequency might be different in Caucasians. *CD74–NRG1* occurred specifically in invasive mucinous lung adenocarcinomas of never smokers, a tumor type that is otherwise associated with *KRAS* mutations (14). In our cohort of limited size (n = 15), *CD74–NRG1* fusions accounted for 27% of invasive mucinous lung adenocarcinomas; together, *KRAS* mutations and *CD74–NRG1* may therefore be considered the causative oncogenes in more than 60% of the cases. We provide evidence that CD74–NRG1 signals through induction of ERBB2–ERBB3 heterodimers, thus leading to PI3K–AKT pathway activation and stimulation of oncogenic growth. In light of the multitude of available drugs targeting ERBB2, ERBB3, and their downstream pathways (19), *CD74–NRG1* fusions may represent a therapeutic opportunity for invasive mucinous lung adenocarcinomas, which frequently present with multifocal and unresectable disease, and for which no effective treatment exists.

METHODS

Sample Preparation, DNA and RNA Extraction, and Illumina Sequencing

Sample preparation and DNA and RNA extraction were performed as previously described (20). RNAseq was performed on cDNA libraries prepared from PolyA+ RNA extracted from tumor cells using the Illumina TruSeq protocol for mRNA. The final libraries were sequenced with a paired-end 2 × 100 bp protocol aiming at 8.5 Gb per sample, resulting in a 30× mean coverage of the annotated transcriptome. All the sequencing was carried on an Illumina HiSeq 2000 sequencing instrument (Illumina).

Analysis of Chromosomal Gene Copy Number (SNP 6.0) and RNAseq Data

Hybridization of the Affymetrix SNP 6.0 arrays was carried out according to the manufacturers' instructions and analyzed using a previously described method (20). For the analysis of RNAseq data, we have developed a pipeline that affords accurate and efficient mapping and downstream analysis of transcribed genes in cancer samples (Fernandez-Cuesta and colleagues; published elsewhere). A brief description of the method was previously provided (20).

Analysis of Targeted Enrichment Genome Sequencing

Genomic DNA was isolated from fresh-frozen tumor tissue and subjected to CAGE Scanner analysis. This approach involves liquid-phase hybrid capture of genomic partitions enriched for genome alterations affecting 333 known cancer-associated genes (also including *CD74*). Subsequent to generation of genomic libraries from tumor DNA and capture, sequencing was performed on the Illumina platform according to the manufacturer's instructions. Significant genomic alterations were identified using approaches described previously (20).

Dideoxy Sequencing

In case of validation, sequencing primer pairs were designed to enclose the putative mutation, or to encompass the candidate rearrangement or chimeric transcript as previously described (20). Sequencing was carried out, and electropherograms were analyzed by visual inspection using four peaks.

Interphase FISH on Formalin-fixed, Paraffin-embedded Sections

Two sets of probes were prepared. One was for break-apart FISH of which probes were mapped at centromeric and telomeric regions between the break point. The other was for fusion FISH that spanned the *NRG1* and *CD74* loci. To intensify the signals, each probe was made of two or three BAC clones as follows, and the probes were labeled with SpectrumGreen and SpectrumOrange (Abbott Molecular-Vysis). Centromeric probes for break-apart FISH were RP11-1002K11 and PR11-25D16. Telomeric probes for break-apart FISH were RP11-23A12 and PR11-715M18. *NRG1* probes for fusion FISH were RP11-715H18, RP11-5713, and PR11-1002K11. *CD74* probes for fusion FISH were PR11-759G10 and PR11-468K14.

Immunohistochemistry

Immunohistochemistry was performed as previously described (21). In brief, the tissue samples were stained with p-ERBB2 (Tyr1221/1222; Cell Signaling Technology) and total ERBB1 (EGFR; Dako) at a dilution of 1:1,000 and 1:50, respectively. The Zeiss MIRAK DESK scanner was used to digitize the stained tissue. Staining for p-EGFR (Tyr1068; Cell Signaling Technology) and p-ERBB3 (Tyr1289; Cell Signaling Technology) was processed with an automated stainer (Autostainer; Dako), using the FLEX+ detection system (Dako).

Cell Culture

H2052, H322, and H1568 cells were obtained from the American Type Culture Collection and maintained in RPMI-1640 medium (Life Technologies) supplemented with 10% fetal calf serum (FCS; Gibco) and 1% penicillin–streptomycin (Gibco). The cells were cultured in a humidified incubator with 5% CO_2 at 37°C. For Western blot analysis experiments, cells were serum starved for 24 hours. NIH-3T3 cells were maintained similarly but in Dulbecco's Modified Eagle Medium (DMEM; Life Technologies). The cells were confirmed to be wild-type for *KRAS*, *EGFR*, *ERBB2*, and *ERBB3* by PCR amplification followed by Sanger sequencing of the PCR products. The cell lines have been authenticated via genotyping (SNP 6.0; Affymetrix) and tested for *Mycoplasma* contamination on a regular basis (MycolAlert; Lonza).

FACS Analysis

NIH-3T3 mouse fibroblast cells were transduced with retrovirus containing empty vector, *CD74–NRG1*, *ERBB2*, *ERBB3*, and *ERBB2+ERBB3*. H2052 cells were transduced with retrovirus

Published OnlineFirst January 27, 2014; DOI: 10.1158/2159-8290.CD-13-0633

containing empty vector or *CD74–NRG1*. Transduced cells (200,000) were washed in fluorescence-activated cell sorting (FACS) buffer (PBS, 2% FCS) and fixed in 4% paraformaldehyde for 30 minutes at room temperature. For permeabilization, cells were washed twice in Saponin buffer (PBS, 0.5% Saponin, and 2% FCS) and intracellular staining of CD74–NRG1 was performed with anti-human–CD74-PE (1:100; BioLegend). Intracellular staining of ERBB2 and ERBB3 was performed with anti-ERBB2 and anti-ERBB3 antibodies (1:50; Cell Signaling Technology). Binding of ERBB2 or ERBB3 was detected with goat–anti-rabbit–Alexa Fluor 488 (Life Technologies). Extracellular staining was performed before permeabilization with anti-human–CD74-PE and anti-NRG1 antibody (1:20; R&D Systems). Binding of the NRG1 part was detected with donkey–anti-goat–Alexa Fluor 488 (Life Technologies). Subsequently, cells were analyzed on a BD LSR II (Beckman Coulter) and quantification was assessed with FlowJo (TreeStar).

Western Blot Analysis

Immunoblotting was performed using standard procedures. The following antibodies were obtained from Cell Signaling Technology: p-AKT Ser473 (Catalog No. #9271), p-P70/S6 (Catalog No. #9205), total ERBB2 (Catalog No. #2242), p-ERBB2 (Catalog No. #2243), total ERBB3 (Catalog No. #4754), and p-ERBB3 (Catalog no. #4791). Anti-human CD74 was obtained from Abcam (Catalog No. # ab22603), and anti-polyclonal NRG1 β 1 was obtained from R&D Systems (Catalog No. AF396-NA). Actin–horseradish peroxidase (HRP) antibody was obtained from Santa Cruz Biotechnology (Catalog No. #sc47778). The antibodies were diluted in 5% BSA/TBST and incubated at 4°C overnight. Proteins were detected with HRP-conjugated anti-mouse, anti-goat, or anti-rabbit antibodies (Millipore) using enhanced chemiluminescence (ECL) reagent (GE Healthcare).

Colony Formation Assay

On a layer of bottom agar (1%), NIH-3T3 cells were suspended at low density in top agar (0.5%) containing 10% FCS, and were grown for 14 days. Subsequently, pictures were taken and systematic analyses were performed with the Scanalyzer (LemnaTec). H1568 cells were cultured under standard conditions in RPMI in 10% FCS and 1% penicillin-streptomycin. p-BABE retroviral vector inserts were confirmed via Sanger sequencing. The cells were generated by at least two independent transductions with retrovirus containing empty vector, *CD74–NRG1*, or *CD74–NRG1_* ΔEGF. After selection for 7 days with puromycin (3 μg/mL), cell lysates were taken for Western blot analysis, and cells were also used for colony formation assays as follows: on a layer of bottom agar (1.2%) cells were suspended at low density in top agar (0.6%) containing 10% FCS (final concentration), and were grown for 14 days. Subsequently, pictures were taken with a Zeiss Axiovert 40 CFL microscope at ×100 magnification, and colony size was assessed with ImageJ (http://rsbweb.nih.gov/ij/).

Generation of Ba/F3_ERBB2+ERBB3 Cells

The *ERBB2* and *ERBB3* open reading frames were amplified by PCR and cloned into the MSCV-puromycin or MSCV-neomycin vectors, respectively (Clonetech). Ba/F3 cells expressing ERBB2 and ERBB3 were generated by retroviral transduction and subsequent puromycin or/and neomycin selection. We verified the expression of the correct proteins by Western blot analysis. Ba/F3 cells were cultured in RPMI-1640 medium supplemented with 10% FBS and 1 ng/mL mouse interleukin-3.

Statistical Analyses

In Fig. 3C and F, we used a two-tailed Fisher exact test.

Disclosure of Potential Conflicts of Interest

L. Fernandez-Cuesta has ownership interest in a patent with the University of Cologne. F. Leenders is a consultant/advisory board member of Blackfield AG. M. Peifer has ownership interest (including patents) in Blackfield AG and is a consultant/advisory board member of the same. F. Malchers is a consultant/advisory board member of One. G.M. Wright has received commercial research support from Covidien and is a consultant/advisory board member of Pfizer. P. Nürnberg is CEO of ATLAS Biolabs GmbH and has ownership interest (including patents) in the same. J.M. Heuckmann is a full-time employee of Blackfield AG and is a co-founder and shareholder of the same. T. Zander is a consultant/advisory board member of Roche, Boehringer Ingelheim, Amgen, and Novartis. R.K. Thomas has received commercial research grants from AstraZeneca, EOS, and Merck KgaA; has ownership interest (including patents) in Blackfield AG and a patent application related to findings in this article; and is a consultant/advisory board member of Blackfield AG, Merck KgaA, Johnson & Johnson, Daiichi-Sankyo, Eli Lilly and Company, Roche, AstraZeneca, Puma, Sanofi, Bayer, Boehringer Ingelheim, and MSD. No potential conflicts of interest were disclosed by the other authors.

Authors' Contributions

Conception and design: L. Fernandez-Cuesta, R.K. Thomas
Development of methodology: L. Fernandez-Cuesta, R. Sun, M. Peifer, J. Altmüller, I. Lahortiga, S. Ogata, M. Parade, D. Brehmer, J. Daßler, S. Ansén, R.K. Thomas
Acquisition of data (provided animals, acquired and managed patients, provided facilities, etc.): L. Fernandez-Cuesta, D. Plenker, H. Osada, R. Menon, F. Leenders, S. Ortiz-Cuaran, M. Bos, J. Daßler, F. Malchers, J. Schöttle, R.T. Ullrich, G.M. Wright, P.A. Russell, Z. Wainer, B. Solomon, H. Nagy-Mignotte, D. Moro-Sibilot, C.G. Brambilla, S. Lantuejoul, J. Altmüller, C. Becker, P. Nürnberg, J.M. Heuckmann, E. Stoelben, J.H. Clement, J. Sänger, L.A. Muscarella, V.M. Fazio, I. Lahortiga, T. Perera, M. Parade, L.C. Heukamp, R. Buettner, T. Zander, J. Wolf, S. Perner, S. Ansén, Y. Yatabe
Analysis and interpretation of data (e.g., statistical analysis, biostatistics, computational analysis): L. Fernandez-Cuesta, D. Plenker, R. Sun, R. Menon, S. Ortiz-Cuaran, F. Malchers, J. Schöttle, R.T. Ullrich, H. Nagy-Mignotte, C.G. Brambilla, J.M. Heuckmann, I. Lahortiga, T. Perera, M. Vingron, J. Wolf, S. Ansén, S.A. Haas, Y. Yatabe, R.K. Thomas
Writing, review, and/or revision of the manuscript: L. Fernandez-Cuesta, D. Plenker, H. Osada, M. Bos, R.T. Ullrich, G.M. Wright, P.A. Russell, Z. Wainer, B. Solomon, E. Brambilla, D. Moro-Sibilot, J. Altmüller, C. Becker, P. Nürnberg, E. Stoelben, D. Brehmer, M. Vingron, R. Buettner, J. Wolf, S. Perner, S. Ansén, Y. Yatabe, R.K. Thomas
Administrative, technical, or material support (i.e., reporting or organizing data, constructing databases): L. Fernandez-Cuesta, D. Plenker, F. Leenders, S. Ortiz-Cuaran, M. Peifer, J. Daßler, F. Malchers, W. Vogel, M. Koker, G.M. Wright, P. Nürnberg, J.M. Heuckmann, I. Petersen, J.H. Clement, J. Sänger, S. Ogata, L.C. Heukamp, R. Buettner, S. Perner, S. Ansén, Y. Yatabe
Study supervision: L. Fernandez-Cuesta, Y. Yatabe, R.K. Thomas
Biobanking of tumor samples: D. Moro-Sibilot
Cell culture work, molecular biological work (e.g., PCR): M. Koker, A. la Torre
Histological review: E. Brambilla, Y. Yatabe
Laboratory work: I. Dahmen
Sample contribution: L.A. Muscarella, A. la Torre

Acknowledgments

The authors are indebted to the patients who donated their tumor specimens as part of the Clinical Lung Cancer Genome

Published OnlineFirst January 27, 2014; DOI: 10.1158/2159-8290.CD-13-0633

Project initiative. Additional biospecimens for this study were obtained from the Victorian Cancer Biobank, Melbourne, Australia. The Institutional Review Board (IRB) of each participating institution approved collection and use of all patient specimens in this study. The authors thank Philipp Lorimier, Marek Franitza, Graziella Bosco, and Juan Luis Fernandez Mendez de la Vega for their technical assistance. The authors also thank the regional computing center of the University of Köln (RRZK) for providing the CPU time on the DFG-funded supercomputer "CHEOPS" as well as for the support.

Grant Support

This work was supported by the Deutsche Krebshilfe as part of the small-cell lung cancer genome-sequencing consortium (grant ID: 109679 to R.K. Thomas, M. Peifer, R. Buettner, S.A. Haas, and M. Vingron); by the EU-Framework Programme CURELUNG (HEALTH-F2-2010-258677 to E. Brambilla, J. Wolf, and R.K. Thomas); by the Deutsche Forschungsgemeinschaft through TH1386/3-1 (to R.K. Thomas); and through SFB832 (TP5 to L.C. Heukamp; and TP6 to R.T. Ullrich, J. Wolf, and R.K. Thomas); by the German Ministry of Science and Education (BMBF) as part of the NGFNplus program (grant 01GS08101 to J. Wolf and R.K. Thomas); by the Deutsche Krebshilfe as part of the *Oncology Centers of Excellence* funding program (to R. Buettner, J. Wolf, and R.K. Thomas); by a Stand Up To Cancer Innovative Research Grant, a Program of the Entertainment Industry Foundation (SU2C-AACR-IRG60109 to R.K. Thomas); by funds of the DFG Excellence Cluster ImmunoSensation (to J. Daßler); by the Italian Ministry of Health (Ricerca Corrente RC1303LO57 and GR Program 2010-2316264) and by the "5 × 1000" voluntary contributions (to L.A. Muscarella); by the Project for Development of Innovative Research on Cancer Therapeutics (P-Direct), Ministry of Education, Culture, Sports, Science and Technology of Japan (to Y. Yatabe); by a research project grant (IWT 110431 to D. Brehmer); by the Belgium government agency for Innovation by Science and Technology (IWT; to I. Lahortiga, S. Ogata, M. Parade, T. Perera, and D. Brehmer); and by Agiradom and French Health Ministry (PPHRC; to C.G. Brambilla).

Received September 13, 2013; revised January 21, 2014; accepted January 23, 2014; published OnlineFirst January 27, 2014.

REFERENCES

1. Pao W, Hutchinson KE. Chipping away at the lung cancer genome. Nat Med 2012;18:349–51.
2. Soda M, Choi YL, Enomoto M, Takada S, Yamashita Y, Ishikawa S, et al. Identification of the transforming *EML4-ALK* fusion gene in non-small-cell lung cancer. Nature 2007;448:561–6.
3. Takeuchi K, Soda M, Togashi Y, Suzuki R, Sakata S, Hatano S, et al. *RET*, *ROS1* and *ALK* fusions in lung cancer. Nat Med 2012;18:378–81.
4. Kohno T, Ichikawa H, Totoki Y, Yasuda K, Hiramoto M, Nammo T, et al. *KIF5B-RET* fusions in lung adenocarcinoma. Nat Med 2012;18:375–7.
5. Lipson D, Capelletti M, Yelensky R, Otto G, Parker A, Jarosz M, et al. Identification of new *ALK* and *RET* gene fusions from colorectal and lung cancer biopsies. Nat Med 2012;18:382–4.
6. Chao BH, Briesewitz R, Villalona-Calero MA. *RET* fusion genes in non-small-cell lung cancer. J Clin Oncol 2012;30:4439–41.
7. Ohashi K, Maruvka YE, Michor F, Pao W. Epidermal growth factor receptor tyrosine kinase inhibitor-resistant disease. J Clin Oncol 2013;31:1070–80.
8. Camidge DR, Bang Y-J, Kwak EL, Iafrate AJ, Varella-Garcia M, Fox SB, et al. Activity and safety of crizotinib in patients with *ALK*-positive non-small-cell lung cancer: updated results from a phase 1 study. Lancet Oncol 2012;2045:11–5.
9. Bergethon K, Shaw AT, Ou S-H, Katayama R, Lovly CM, McDonald NT, et al. *ROS1* rearrangements define a unique molecular class of lung cancers. J Clin Oncol 2012;30:863–70.
10. Shaw AT, Kim D-W, Nakagawa K, Seto T, Crinó L, Ahn M-J, et al. Crizotinib versus chemotherapy in advanced *ALK*-positive lung cancer. New Engl J Med 2013;368:2385–94.
11. Hynes NE, Lane HA. ERBB receptors and cancer: the complexity of targeted inhibitors. Nat Rev Cancer 2005;5:341–54.
12. Mei L, Xiong W. Neuregulin 1 in neural development, synaptic plasticity and schizophrenia. Nat Rev Neurosci 2008;9:437–52.
13. Talmage DA. Mechanisms of neuregulin action. Novartis Found Symp 2008;289:74–84.
14. Maeda Y, Tsuchiya T, Hao H, Tompkins DH, Xu Y, Mucenski ML, et al. $KRAS^{G12D}$ and NKX2-1 haploinsufficiency induce mucinous adenocarcinoma of the lung. J Clin Invest 2012;122:4388–400.
15. Falls D. Neuregulins: functions, forms, and signaling strategies. Exp Cell Res 2003;284:14–30.
16. Wallasch C, Weiss FU, Niederfellner G, Jallal B, Issing W, Ullrich A. Heregulin-dependent regulation of HER2/neu oncogenic signaling by heterodimerization with HER3. EMBO J 1995;14:4267–75.
17. Imielinski M, Berger AH, Hammerman PS, Hernandez B, Pugh TJ, Hodis E, et al. Mapping the hallmarks of lung adenocarcinoma with massively parallel sequencing. Cell 2012;150:1107–20.
18. The Clinical Lung Cancer Genome Project (CLCGP), Network Genomic Medicine (NGM). A genomics-based classification of human lung tumors. Sci Transl Med 2013;5:209ra153.
19. Yarden Y, Pines G. The ERBB network: at last, cancer therapy meets systems biology. Nat Rev Cancer 2012;12:553–63.
20. Peifer M, Fernández-Cuesta L, Sos ML, George J, Seidel D, Kasper LH, et al. Integrative genome analyses identify key somatic driver mutations of small-cell lung cancer. Nat Genet 2012;44:1104–10.
21. Wilbertz T, Wagner P, Petersen K, Stiedl A-C, Scheble VJ, Maier S, et al. *SOX2* gene amplification and protein overexpression are associated with better outcome in squamous cell lung cancer. Mod Pathol 2011;24:944–53.